

The thrombospondin repeat containing protein MIG-21 controls a left–right asymmetric Wnt signaling response in migrating *C. elegans* neuroblasts

Teije C. Middelkoop^a, Lisa Williams^b, Pei-Tzu Yang^a, Jeroen Luchtenberg^a, Marco C. Betist^a, Ni Ji^c, Alexander van Oudenaarden^c, Cynthia Kenyon^b, Hendrik C. Korswagen^{a,*}

^a Hubrecht Institute, Royal Netherlands Academy of Arts and Sciences and University Medical Center Utrecht, Uppsalalaan 8, 3584 CT, Utrecht, The Netherlands

^b Department of Biochemistry and Biophysics, University of California San Francisco, San Francisco, CA 94158-2517, USA

^c Department of Physics and department of Biology, Massachusetts Institute of Technology, 77 Massachusetts Avenue, Cambridge, MA 02139, USA

ARTICLE INFO

Article history:

Received for publication 6 July 2011

Revised 13 October 2011

Accepted 24 October 2011

Available online 29 October 2011

Keywords:

C. elegans

Wnt

Cell migration

Signal transduction

Cell polarity

ABSTRACT

Wnt proteins are secreted signaling molecules that play a central role in development and adult tissue homeostasis. Although several Wnt signal transduction mechanisms have been described in detail, it is still largely unknown how cells are specified to adopt such different Wnt signaling responses. Here, we have used the stereotypic migration of the *C. elegans* Q neuroblasts as a model to study how two initially equivalent cells are instructed to activate either β -catenin dependent or independent Wnt signaling pathways to control the migration of their descendants along the anteroposterior axis. We find that the specification of this difference in Wnt signaling response is dependent on the thrombospondin repeat containing protein MIG-21, which acts together with the netrin receptor UNC-40/DCC to control an initial left–right asymmetric polarization of the Q neuroblasts. Furthermore, we show that the direction of this polarization determines the threshold for Wnt/ β -catenin signaling, with posterior polarization sensitizing for activation of this pathway. We conclude that MIG-21 and UNC-40 control the asymmetry in Wnt signaling response by restricting posterior polarization to one of the two Q neuroblasts.

© 2011 Elsevier Inc. All rights reserved.

Introduction

Wnt proteins are members of an evolutionarily conserved family of signaling molecules that play a central role in the development of multicellular organisms, controlling processes as diverse as cell fate specification, polarization and migration (Cadigan and Nusse, 1997). Wnt proteins mediate these different functions by triggering distinct signaling pathways, such as the canonical Wnt/ β -catenin pathway, which controls the expression of specific sets of target genes and β -catenin independent pathways (collectively referred to as non-canonical Wnt signaling pathways), which mediate the function of Wnt in cell polarization and migration (Clevers, 2006; Schlessinger et al., 2009). Although some of these signaling pathways have been described in detail, much less is known about how cells are specified to respond to Wnt through such different signaling mechanisms.

Here we use the migration of the *C. elegans* Q neuroblasts as a model to study how differences in the response to Wnt are specified *in vivo*. At the end of embryogenesis, two Q neuroblasts are generated at equivalent left–right positions within the two lateral rows of hypodermal seam cells (Fig. 1A, B) (Sulston and Horvitz, 1977). During the first hours of larval development, the Q neuroblasts polarize and

migrate in opposite directions – the left Q neuroblast (QL) migrates posteriorly, whereas the right Q neuroblast (QR) migrates anteriorly. While migrating along the anteroposterior axis, both Q neuroblasts undergo an identical pattern of cell divisions, each generating 3 descendants (Q,d) that move toward well-defined final positions and differentiate into neurons (Fig. 1A, B).

Several studies have shown that the left–right asymmetry in Q,d migration is controlled by Wnt signaling (Korswagen et al., 2000; Maloof et al., 1999; Whangbo and Kenyon, 1999; Zinovyeva et al., 2008). Just prior to the first division of the Q neuroblasts, the posteriorly expressed Wnt protein EGL-20 activates a canonical Wnt/ β -catenin signaling pathway in QL. This results in the expression of the Antennapedia-like Hox gene *mab-5*, which is necessary and sufficient for the subsequent posterior migration of the QLd (Fig. 1A) (Harris et al., 1996; Salser and Kenyon, 1992). EGL-20 does not activate *mab-5* expression in QR and as a consequence, the QR,d migrate in the default anterior direction (Fig. 1B). This anterior migration is also EGL-20 dependent, but here EGL-20 acts together with other Wnt proteins through a β -catenin independent signaling pathway to guide the QR,d to their precisely defined final positions (Zinovyeva et al., 2008). The left–right asymmetric response to EGL-20 is intrinsic to the Q neuroblasts and depends on a difference in activation threshold for the EGL-20 dependent expression of *mab-5* (Whangbo and Kenyon, 1999). Thus, in dose response experiments using inducible EGL-20 expression in an *egl-20* mutant background, both QL and QR activate canonical Wnt/ β -catenin signaling

* Corresponding author. Fax: +31 30 2516464.

E-mail address: r.korswagen@hubrecht.eu (H.C. Korswagen).

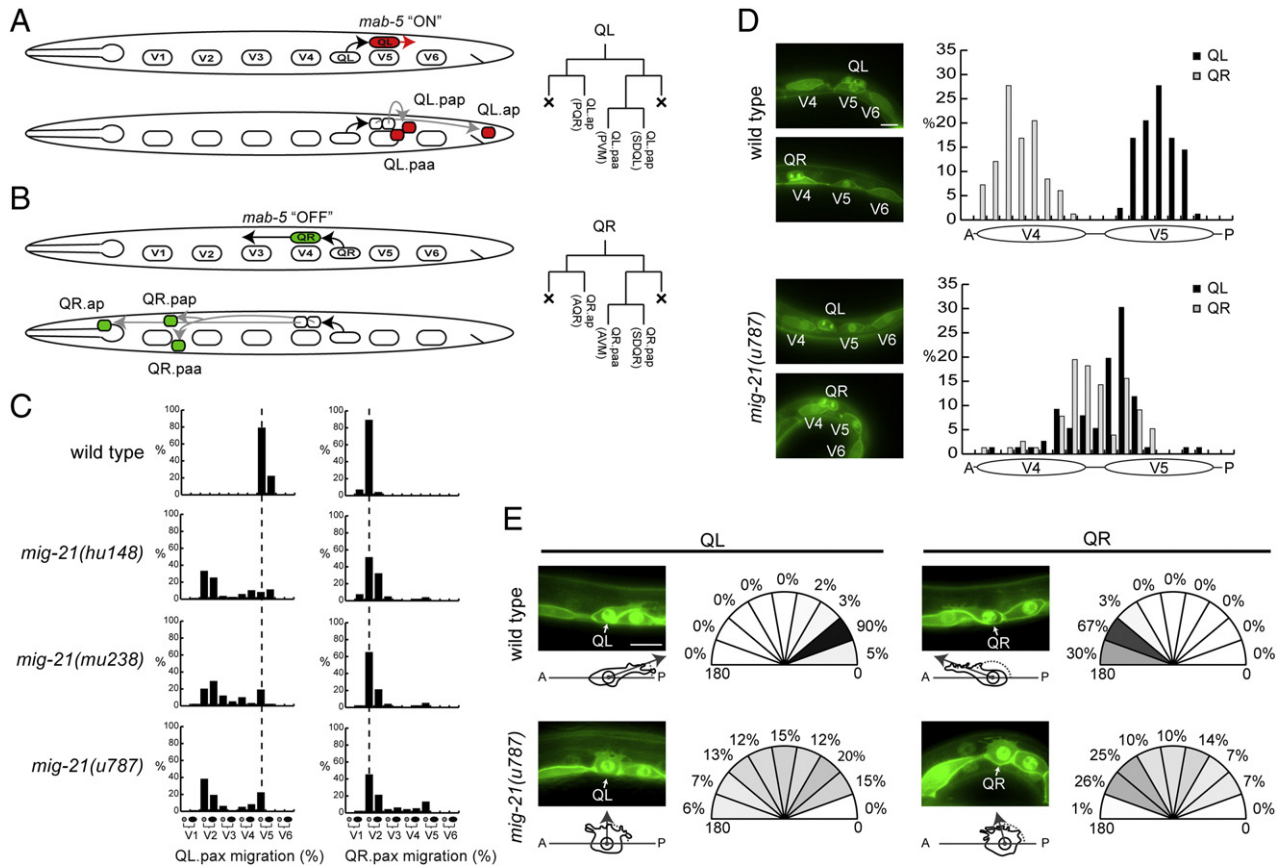


Fig. 1. *mig-21* controls Q cell migration. (A–B) Schematic overview of initial Q neuroblast migration (top panels) and Q descendant (Q.d) migration (lower panels) of the QL (A) and QR (B) lineage in wild type L1 larvae. On the left lateral side QL migrates over its neighboring seam cell V5 during the first 4 h of L1 development (A, top), whereas QR migrates over seam cell V4 (B, top). At the end of the initial migration stage, QL expresses the Wnt target gene *mab-5*. After the initial migration, the Q neuroblasts undergo an identical pattern of cell division, each generating 3 descendants that migrate long distances along the anteroposterior axis. QL.d cells express *mab-5* and migrate posteriorly (A, bottom) while QR.d cells do not express *mab-5* and migrate anteriorly (B, bottom). At the end of L1, Q.d cells are localized at well-defined final positions along the anteroposterior axis. Lineage diagrams of QL (A) and QR (B) are shown on the right. Crosses indicate apoptotic cells. (C) Quantification of the final position of QR.pax and QL.pax as scored with respect to the stationary seam cells V1–V6 in wild type and in 3 different alleles of *mig-21* ($n > 80$ for each genotype). In *mig-21(u787)* no significant difference between the final position of QL.pax and QR.pax was found ($p > 0.3$, Fisher's exact test). Dashed lines indicate wild type Q.d positions. (D) Quantification of the position of the Q neuroblast nuclei with respect to seam cell V4 and V5 after initial migration ($n > 70$). For this assay animals carrying *Pwrt-2::gfp-ph*; *Pwrt-2::h2b-gfp (hels63)* were analyzed. Images on the left are representative epifluorescent micrographs showing GFP-PH and H2B-GFP expressed in seam cells and Q cells. (E) Quantification of the direction of Q cell polarization 1–2 h after hatching in *hels63*. The angle of the main protruding front with the anteroposterior axis (varying from 0° – 180°) was measured and displayed in a radial diagram ($n \geq 60$ for both genotypes). Note that ventral protrusions (180° – 360°) were never observed. Images on the left are representative epifluorescent micrographs. Illustrations show the vectors drawn and dashed lines indicate the angle depicted in the radial diagrams. Scale bars represent $5 \mu\text{m}$ for all micrographs. Anterior is left, dorsal is up.

and *mab-5* expression at high EGL-20 levels, whereas only QL activates the pathway at a lower EGL-20 dose (Whangbo and Kenyon, 1999).

Unlike the migration of the Q descendants, the initial polarization and short-range migration that precedes the first Q neuroblast division is independent of Wnt signaling (Chapman et al., 2008; Harris et al., 1996). To date, several mutations have been identified that show defects in this initial left–right asymmetry, including *dpy-19*, *unc-40/DCC* and *mig-15/NIK* kinase (Chapman et al., 2008; Honigberg and Kenyon, 2000). Upon loss of these genes, the direction of initial Q neuroblast polarization and migration becomes random on both the left and right side. Similarly, both the QL.d and QR.d migrate either anteriorly or posteriorly, suggesting that they randomly activate canonical Wnt/ β -catenin signaling. In support of this hypothesis is the finding that *mab-5* expression in the Q neuroblasts is randomized in *dpy-19* and *unc-40* mutants (Honigberg and Kenyon, 2000) and that mutation of *mab-5* prevents posterior migration of the Q cell descendants in these mutants (Chapman et al., 2008; Honigberg and Kenyon, 2000). Based on these results, a model has been proposed in which posterior polarization of the Q neuroblasts during the initial asymmetric polarization and migration stage sensitizes the Q neuroblasts for EGL-20 induced canonical Wnt/ β -catenin signaling (Chapman et al., 2008; Honigberg and Kenyon, 2000). Experimental evidence confirming this model is however still lacking.

Here, we show that the previously identified locus *mig-21*, which is required for the initial polarization and migration of the Q neuroblasts (Du and Chalfie, 2001), encodes a thrombospondin repeat containing transmembrane protein. *mig-21* acts cell autonomously within the Q neuroblasts and genetically interacts with the netrin receptor *unc-40/DCC* to control the initial polarization of the Q neuroblasts. By performing EGL-20 dose response experiments, we demonstrate that *mig-21* is required for the difference in EGL-20 response threshold of QL and QR. Importantly, we show by single molecule mRNA fluorescence in situ hybridization (smFISH) that at the end of the initial polarization and migration process, the position of the Q neuroblasts along the anteroposterior axis correlates with the expression level of *mab-5*. Thus, in *mig-21* mutants, in which the positioning of the QL and QR cells is random, the most posteriorly localized cells express the highest levels of *mab-5*. Furthermore, *mab-5* expression is lost in *unc-40; mig-21* double mutants, in which the Q neuroblasts fail to polarize and migrate toward the posterior. Taken together, our results demonstrate that polarization and migration toward the posterior lowers the threshold for EGL-20 dependent Wnt/ β -catenin signaling and *mab-5* expression. We conclude that *mig-21*, together with *unc-40*, controls the left–right asymmetry in the response to EGL-20 by restricting posterior polarization to QL and anterior polarization to QR.

Materials and methods

C. elegans strains and culture

Unless stated otherwise, *C. elegans* strains were grown at 20 °C using standard culture conditions. The Bristol N2 strain was used as wild type. Mutant alleles and transgenes used in this study are LGI: *dpy-5(e61) unc-40(e1430)*; LGII: *muls32[Pmec-7::gfp; lin-15(+)]* (Ch'ng et al., 2003); LGIII: *mig-21(u787)*, *mig-21(mu238)*, *mig-21(hu148)*, *dpy-19(e1259)*; LGIV: *egl-20(n585)*; LGV: *hels63[Pwrt-2::gfp-ph; Pwrt-2::h2b-gfp; Plin-48::tomato]* (M. Wildwater and S. van den Heuvel, personal communication), *muls53[hs::egl-20; unc-22(dn)]* (Whangbo and Kenyon, 1999) and the extra-chromosomal transgene *huEx260[Pegl-17::mig-21; Pmyo-2::gfp]*. Mutagenesis was performed on *muls32[Pmec-7::gfp; lin-15(+)]* animals (Ch'ng et al., 2003) using ethylmethane sulfonic acid (EMS) as described (Brenner, 1974). *mig-21(mu238)* and *mig-21(hu148)* were isolated in independent mutagenesis screens and were three times backcrossed with the Bristol N2 wild type strain. Synchronization of animals was performed by collecting L1 larvae that hatched within a specific time interval. Animals carrying *unc-40(e1430)* were synchronized by bleach treatment.

Phenotypic analysis and microscopy

The positions of the Q descendants QL.pap-QL.paa and QR.pap-QR.paa were scored by DIC microscopy in late L1 stage larvae as described (Coudreuse et al., 2006). The position of the Q neuroblasts after initial migration was determined in animals 4–5 hours post-hatching by scoring the position of the Q neuroblast nucleus with respect to the nuclei of the seam cell V4 and V5. The normalized position of the Q neuroblast was determined by dividing the distance between the V4 nucleus and the Q nucleus by the distance between the V4 nucleus and the V5 nucleus. Only animals were included in which at least one Q neuroblast was either in mitosis or had just divided.

The direction of initial Q polarization was determined by scoring the angle of the main protruding front of the Q cell with respect to the anteroposterior axis in 1–2 hour synchronized animals. The main protruding front was defined as the area between the two most lateral filopodia. Q neuroblast positioning and polarization assays were performed using epifluorescence imaging on animals carrying *hels63*. For epifluorescence and DIC imaging animals were mounted on 2% agarose pads containing 10 mM sodium azide. Micrographs were made using a Zeiss Axioscop microscope equipped with a Zeiss AxioCam digital camera.

Time lapse imaging

For time lapse imaging, synchronized animals (0–1 h after hatching) were mounted in 0.5 µl of 0.1 µm diameter polystyrene microparticles in aqueous suspension (Polysciences 00876 2.5% w/v aqueous suspension) onto a 10% agarose patch (Christopher Fang-Yen, personal communication). Animals were imaged using a Leica TCS SPE confocal microscope (63× objective, zoom 2.5×, 6% 488 nm laser power). Z-stacks were made (0.5 µm step size) every 30 min for 7 h. Image acquisition was performed using LASAF software. Z-slices in which the Q cell nucleus was in focus were selected. Images were processed and movies were generated using Adobe Photoshop and ImageJ respectively.

Positional cloning and molecular characterization of *mig-21*

mig-21 was mapped to LGIII between the Tc1 markers stP19 and stP120 using a PCR-based transposon mapping method (Williams et al., 1992). Deficiency analysis placed *mu238* between the deficiencies sDf121 and sDf125. The genetic endpoints of these deficiencies placed *mu238* between the genes *daf-4* (−1.53) and *let-774* (−1.42). This position was confirmed with a 3-factor cross between *mig-21(mu238)* and *dpy-17(e164) unc-32(e189)*. 19/49 Dpy nUnc recombinants

segregated Mig progeny, and 41/63 Unc nDpy recombinants segregated Mig progeny. These data placed *mig-21(mu238)* at approximately −1.34 and −1.43, respectively.

Cosmids were provided by A. Coulson of the Wellcome Trust Sanger Institute (Cambridge, UK) and J. Sulston of the Medical Research Council (Cambridge, UK). The region between *daf-4* and *let-774* was covered by 18 cosmids. Cosmid pools spanning this interval were injected into *mig-21(mu238)* animals using pTG96 (*sur-5::gfp*) (Gu et al., 1998) as a co-injection marker, and F2 and F3 progeny of F1 transformants were assayed for rescue of the QL.pax phenotype. Partial rescue was obtained from injection of the cosmid F01F1, and this rescuing activity was narrowed to a 7.5 kb PCR product that contains the predicted genes F01F1.2 and F01F1.13. Each lesion was identified in more than one independent PCR product.

Part of the predicted *mig-21* cDNA, including the 3' UTR, was amplified by 3' RACE RT-PCR. Sequence analysis revealed differences with the predicted gene structure in Wormbase, leading to an additional 3' coding sequence (NCBI accession number JN165085). Various attempts to amplify the predicted 5' end of the *mig-21* ORF were unsuccessful. For tissue specific rescue experiments, *mig-21* genomic sequence was amplified using 5'-ATGAGCGCGACTCTAAC-3' and 5'-TCACCAAAACTT-TCATCTTCGGG-3' and sub-cloned into pJET1.2. To obtain *Pegl-17*, 4.6 kb of sequence upstream of the *egl-17* coding sequence was PCR amplified. Next, *Pegl-17*, *mig-21* and the *unc-54-3'* UTR were cloned using Gateway technology into pDONRP4-P1R, pDONR221 and pDONRP2R-P3 entry clones respectively. *Pegl-17::mig-21::unc-54-3'UTR* (pKN162) was generated by 3-way Gateway cloning into the destination vector pKN133. *Pegl-17::mig-21::unc-54-3'UTR* was injected at 20 ng/µl together with 8 ng/µl of *Pmyo-2::GFP* and 120 ng/µl pBluescript II as carrier DNA into *mig-21(u787)*.

An RNAi clone of F01F1.13 was obtained from the Ahringer RNAi library and analyzed as described (Kamath and Ahringer, 2003; Kamath et al., 2003). Q.d migration was assayed with a Leica MZFLIII stereomicroscope by examining the position of AVM (QR.paa) and PVM (QL.paa) with respect to the vulva in *muls32[Pmec-7::gfp; lin-15(+)]* animals.

Heat shock experiments

Heat shock experiments were performed on animals carrying *muls53[hs::egl-20; unc-22(dn)]* as described (Whangbo and Kenyon, 1999). Briefly, heat shock treatment was given to 0–0.5 hour synchronized L1 larvae in a total volume of 50 µl at 33 °C for 0 min (control), 2 min or 7 min. To terminate the heat shock treatment, tubes were chilled on ice for 10 s. After heat shock, animals were put on fresh plates and grown at 15 °C for 12 h and at 20 °C for 4–6 h. Final Q descendent positions were scored at the late L1 stage.

Single molecule fluorescence in situ hybridization

smFISH was performed as described (Raj et al., 2008). In short, synchronized L1 animals were fixed using 4% formaldehyde and 70% ethanol. Hybridization was done for >12 h at 30 °C in the dark. Oligonucleotide probes were designed using a specific algorithm (www.singlemoleculfish.com) and chemically coupled to Alexa594 (*mab-5* probe) or Cy5 (*mig-21* probe). Before mounting, hybridized animals were washed in the presence of DAPI for nuclear counterstaining. z-stacks of 0.5 µm slice thickness were collected using a Leica DM6000 microscope equipped with a Leica DFC360FX camera, 100× objective, Tx2 filter cube (Alexa594) or an Y5 filter cube (Cy5). Images with 1024×1024 resolution were subjected to 2×2 binning and were further analyzed with ImageJ.

For quantification, z-stacks were used. Quantification was performed by manually counting mRNA spots in Q neuroblasts of animals that carried the *hels63* transgene to mark the Q cell periphery. Only fluorescent spots that were visible in at least two neighboring z-slices were counted to eliminate false positive signals.

Statistical analysis

Data are represented as mean \pm standard deviation of the indicated number (n) of independent experiments. To assess the correlation between *mab-5* transcript level and Q neuroblast position in *mig-21* mutants, we calculated the Spearman's rank correlation coefficients (see main text for exact values). Furthermore, we performed robust linear regression (robustfit function in Matlab) to test whether a simple linear model could explain such correlation. This robust regression method effectively minimizes the influence of data outliers and yielded the best fit lines for both Q neuroblasts.

Results

mig-21 is required for the left–right asymmetry in Q descendant migration

To gain further insight into the mechanism controlling the left–right asymmetry in Q neuroblast migration, we characterized two alleles, *hu148* and *mu238*, that were isolated in genetic screens for mutations that disrupt the stereotypic migration of the Q cell descendants. In *hu148* and *mu238*, the QL descendants QL.paa and QL.pap (here referred to as QL.d) localize either at their normal position in the posterior or at a position in the anterior that corresponds to the final position of the QR.d in wild type animals (Fig. 1C). Also in case of the QR.d, the cells sometimes localize at a position in the posterior normally taken by the QL.d, indicating that the left–right asymmetry in Q descendant migration is partially disrupted in *hu148* and *mu238*. Complementation tests showed that *hu148* and *mu238* are allelic to the previously identified locus *mig-21* (as defined by the allele *u787*) (Du and Chalfie, 2001). As *u787* showed the most penetrant defect in Q descendant positioning (Fig. 1C), we focused on this allele for further analysis.

mig-21 controls the initial polarization and migration of the Q neuroblasts

It has previously been observed that in addition to the defect in Q descendant migration, *mig-21* mutants also show mispositioning of the QL and QR neuroblasts during the initial short range migration that precedes the Wnt dependent migration of their descendants (Du and Chalfie, 2001). To extend these observations, we imaged Q neuroblast polarization and migration at high resolution using a marker that outlines the cell periphery (GFP-PH, a Pleckstrin homology domain containing GFP which is targeted to the plasma membrane) and a marker that labels the nucleus (H2B-GFP). Importantly, neither of these markers influences the normal polarization and migration of the Q neuroblasts and their descendants (Fig. S1). During the first 4–5 h after hatching, QR migrates toward the anterior and divides once it reaches a position above the seam cell V4. In the same time frame, QL migrates toward the posterior and divides at a position above V5 (Fig. 1D) (Sulston and Horvitz, 1977). We found that in *mig-21* mutants the initial migration was often shorter than in wild type animals, with Q neuroblasts dividing at positions in between V4 and V5. In addition, a subset of QL and QR neuroblasts migrated in the opposite direction (Fig. 1D), confirming the earlier observation that the initial left–right asymmetric positioning of the Q neuroblasts is defective in *mig-21* mutants (Du and Chalfie, 2001).

The initial migration of the Q neuroblasts is preceded by a left–right asymmetric polarization of the cells that commences shortly after hatching. During this time, QL sends out a protrusion toward the posterior, which extends over V5, while QR polarizes in the opposite direction, with the protrusion extending over V4 (Fig. 1E). Using the GFP-PH marker, we also observed smaller, spike-like filopodia, which were mostly restricted to the leading edge of the main protrusion of QL and QR. We found that in *mig-21* mutants these filopodia were often present at multiple sites along the dorsal surface of the Q neuroblasts. Furthermore, the overall polarization direction of QL and QR was no longer restricted toward one direction (Fig. 1E). To

quantify the direction of polarization, a vector was drawn from the Q cell nucleus to the center of the protruding front and the angle of this vector with the anteroposterior axis was measured. In wild type animals, the average angle was $29.9 \pm 7.5^\circ$ (mean \pm SD, $n = 62$) for QL and $156.3 \pm 7.1^\circ$ for QR ($n = 60$). In *mig-21* mutants, the direction of polarization was highly variable, with an average angle of $86.7 \pm 41.8^\circ$ for QL ($n = 68$) and $109.2 \pm 37.9^\circ$ for QR ($n = 72$), indicating that *mig-21* is required for the initial left–right asymmetric polarization of the Q neuroblasts (Fig. 1E).

To examine the spatiotemporal dynamics of the initial polarization and migration process, we performed *in vivo* time lapse imaging. In wild type animals, the Q neuroblasts first form a protrusion that extends to a position over the neighboring seam cell (Movie 1A–B). Next, the Q neuroblasts detach from the row of seam cells and the cell body follows the protruding front, ultimately positioning QR above V4 and QL above V5. Importantly, the direction of the protrusion is maintained over time and is always pointed toward the anterior (QR) or posterior (QL) and the small filopodia are only formed at the protruding front. In contrast, we found that the direction of the protruding front changed repeatedly in *mig-21* mutants. Furthermore, dynamic ectopic filopodia were often formed in multiple directions along the dorsal surface of the cell (Movie 1C–D). Despite these differences, the Q neuroblasts detached normally from the row of seam cells and divided in the same time frame as observed in wild type animals. Taken together, our results suggest that *mig-21* is not required for the formation of protrusions or for the capacity of the Q neuroblasts to migrate. Instead, we conclude that *mig-21* restricts the direction of polarization and thereby controls the initial left–right asymmetric migration of the Q neuroblasts.

mig-21 functions in parallel with the netrin receptor *unc-40/DCC* in Q neuroblast polarization and migration

It has previously been shown that mutants of the netrin receptor *unc-40/DCC* display defects in the initial polarization and migration of the Q neuroblasts (Honigberg and Kenyon, 2000). Quantification of Q neuroblast position after initial migration in the *unc-40* null allele *e1430* showed a more wide-spread distribution of QL and QR, together with a reduction in the extent of posterior and anterior migration (Fig. 2A). Although less pronounced, this phenotype is similar to what we observed in *mig-21* mutants. To investigate the functional relationship between *mig-21* and *unc-40*, we assayed initial Q neuroblast migration in *unc-40; mig-21* double mutants. In contrast to the *mig-21* and *unc-40* single mutants, which show a distribution of QL and QR cells that extends to the anterior side of the seam cell V5, there was a strong reduction in posterior migration in the *unc-40; mig-21* double mutant, with most cells localizing around the posterior side of V4 (Fig. 2A). Furthermore, we found that the overall distribution of the QL and QR neuroblasts along the anteroposterior axis became similar, with a clear truncation of both the anterior and posterior sides of the spectrum. The strong additive effect of the double mutant suggests that *mig-21* and *unc-40* act in parallel genetic pathways to mediate the left–right asymmetric polarization of the Q neuroblasts.

mig-21 encodes a single pass transmembrane protein with two extracellular thrombospondin repeats

mig-21 was cloned using standard positional mapping and transformation rescue experiments (see Materials and methods) and was shown to correspond to the predicted gene F01F1.13 (Fig. S2). Consistently, RNAi using the F01F1.13 coding sequence phenocopied the *mig-21* mutant phenotype (in 51% of the animals, the QL.d localized in the anterior and in 3% the QR.d localized in the posterior, $n > 100$). To determine the molecular lesions of *hu148*, *mu238* and *u787*, we sequenced the genomic region of F01F1.13 and identified

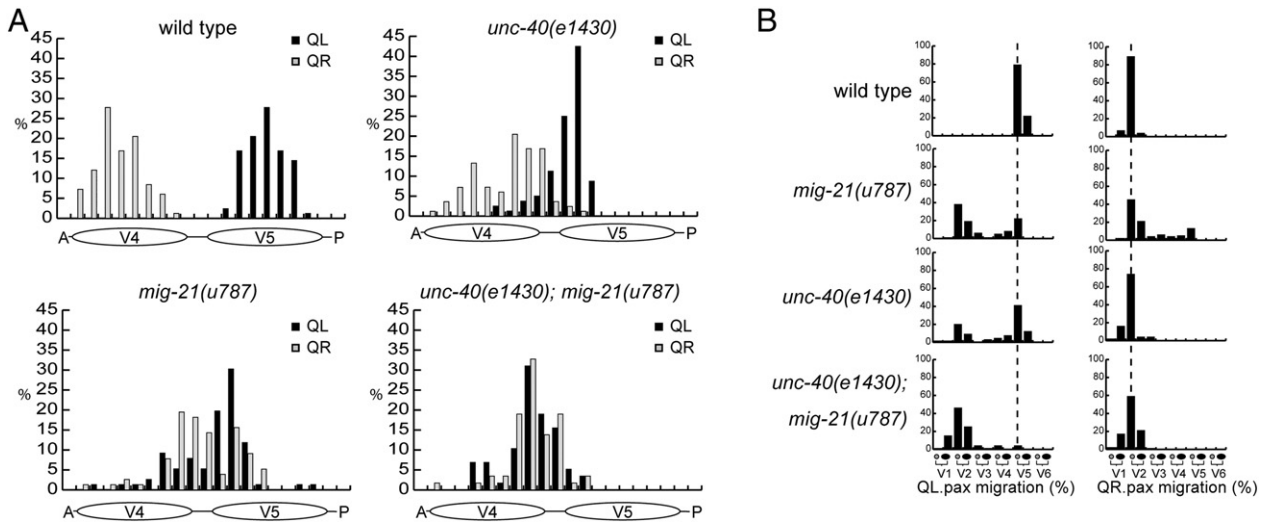


Fig. 2. *mig-21* enhances the Q cell migration defects of *unc-40*. (A) Quantification of the position of the Q neuroblast nuclei with respect to the seam cells V4 and V5 after initial migration but before Q daughter cell migration in wild type, *mig-21*, *unc-40* and *unc-40*; *mig-21* (for wild type, *mig-21* and *unc-40* $n > 70$, for *unc-40*; *mig-21* $n \geq 50$). Q cell position after initial migration differs significantly between *unc-40*, *mig-21* singles and the *unc-40*; *mig-21* double mutant (Fisher's exact test, $p < 0.001$ for both QL and QR). (B) Quantification of the final positions of the Q.pax cells with respect to the stationary seam cells in wild type, *mig-21*, *unc-40* and *unc-40*; *mig-21* (for wild type, *mig-21* and *unc-40*; *mig-21* $n > 80$, for *unc-40* $n \geq 50$). The final position of Q.d cells on the anteroposterior axis differs significantly between *unc-40* and *mig-21* single mutants and the *unc-40*; *mig-21* double mutant (Fisher's exact test, $p < 0.001$ for both QL and QR). Dashed lines indicate the final position of Q.d cells in wild type.

mutations for all three alleles, with *u787*, *hu148* and *mu238* introducing stop codons at W58, W115 and W208, respectively (Fig. 3, S2). Amplification of F01F1.13 cDNA fragments (see **Materials and methods**) revealed a splicing pattern that differs from the predicted gene model in Wormbase and results in additional sequence at the carboxy-terminus of F01F1.13. From here on, we will refer to F01F1.13 as *mig-21*.

mig-21 encodes a single pass transmembrane protein with two extracellular thrombospondin type I (TSP-I) repeats (Fig. 3), a protein motif that is also found in UNC-5 and members of the Semaphorin family and is often associated with cell and axon guidance functions in neuronal development (Adams and Tucker, 2000). Apart from the two TSP-I repeats, sequence similarity searches did not reveal other conserved domains in MIG-21 and no orthologs were found outside the nematode phylum. Although MIG-21 shares a TSP-I motif with UNC-5, a receptor that functions together with UNC-40/DCC in UNC-6/Netrin signaling (Wadsworth, 2002), our results indicate that *mig-21* and *unc-40* function in parallel genetic pathways in Q neuroblast polarization and migration.

mig-21 functions cell autonomously in the Q neuroblasts during initial polarization and migration

To examine the expression pattern of *mig-21*, we used single molecule mRNA FISH (smFISH) (Raj et al., 2008) to quantitatively determine *mig-21* transcript localization and levels in L1 stage larvae. Using this technique, single transcripts are visualized as bright diffraction limited spots by hybridizing 48 or more short fluorescently labeled probes to the mRNA of interest. We found that *mig-21* is symmetrically expressed between the two Q neuroblasts. This expression is however transient

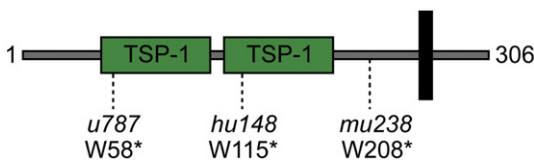


Fig. 3. Schematic view of the MIG-21 protein. *mig-21* encodes a single pass transmembrane protein with two extracellular thrombospondin-I (TSP-I) repeats. Molecular lesions of the 3 alleles described in this study are shown. *u787* and *hu148* introduce early stop codons, truncating the protein at the first and second TSP-I repeat, respectively. *mu238* introduces an early stop codon after the second TSP-I repeat.

and restricted to the time period in which the initial polarization and migration of the Q neuroblasts takes place. Thus, within the first two hours after hatching, when the Q neuroblasts have polarized but the cell body has not yet migrated, an average of 25 ± 4.6 *mig-21* transcripts (mean \pm SD, $n = 12$) were found in QL and 26 ± 5.0 transcripts in QR ($n = 17$) (Fig. 4A). At 2–4 h after hatching, when the Q neuroblasts are migrating over their neighboring seam cells, expression decreased slightly, with 17 ± 5.8 *mig-21* transcripts in QL ($n = 15$) and 21 ± 6.2 transcripts in QR ($n = 18$) (Fig. 4B). Four to six hours after hatching, when the Q neuroblasts have divided, *mig-21* expression was strongly decreased, with 2 ± 2.4 transcripts in QL ($n = 22$) and 5 ± 3.4 transcripts in QR ($n = 19$) (Fig. 4C). In addition to the expression in the Q neuroblasts, *mig-21* is also expressed in the four body wall muscle quadrants of L1 stage larvae (Fig. 4D and data not shown). In contrast to the expression in the Q neuroblasts, the muscle specific expression of *mig-21* persists throughout development.

The transient expression of *mig-21* in the Q neuroblasts during initial polarization and migration suggests a cell autonomous function of *mig-21* in this process. To investigate whether expression of *mig-21* in the Q neuroblasts is sufficient for the function of *mig-21* in Q cell polarization and migration, we expressed wild type *mig-21* using the *egl-17* promoter in *mig-21* mutants. At the L1 stage of larval development, the *egl-17* promoter is expressed in the Q neuroblasts and in a subset of cells in the head (Branda and Stern, 2000; Cordes et al., 2006). Importantly, the *egl-17* promoter is not expressed in body wall muscle cells, as confirmed by smFISH analysis of *mig-21(u787)*; *Pegl-17::mig-21* animals, which showed clear overexpression of *mig-21* in the Q neuroblasts but not in body wall muscle cells (Fig. 5B). We found that Q neuroblast specific expression of *mig-21* almost fully rescued the *mig-21* mutant phenotype (Fig. 5A), consistent with a cell autonomous function of *mig-21* in the Q neuroblasts. Furthermore, in line with the mutant phenotype, the transient expression of *mig-21* suggests that it is specifically required during initial Q neuroblast migration.

mig-21 controls the left–right asymmetric response to EGL-20/Wnt

Once the initial polarization and migration are complete, QL responds to the Wnt ligand EGL-20 by activating a canonical Wnt/ β -catenin pathway (Korswagen et al., 2000; Maloof et al., 1999). This leads to expression of the target gene *mab-5*, which in turn directs

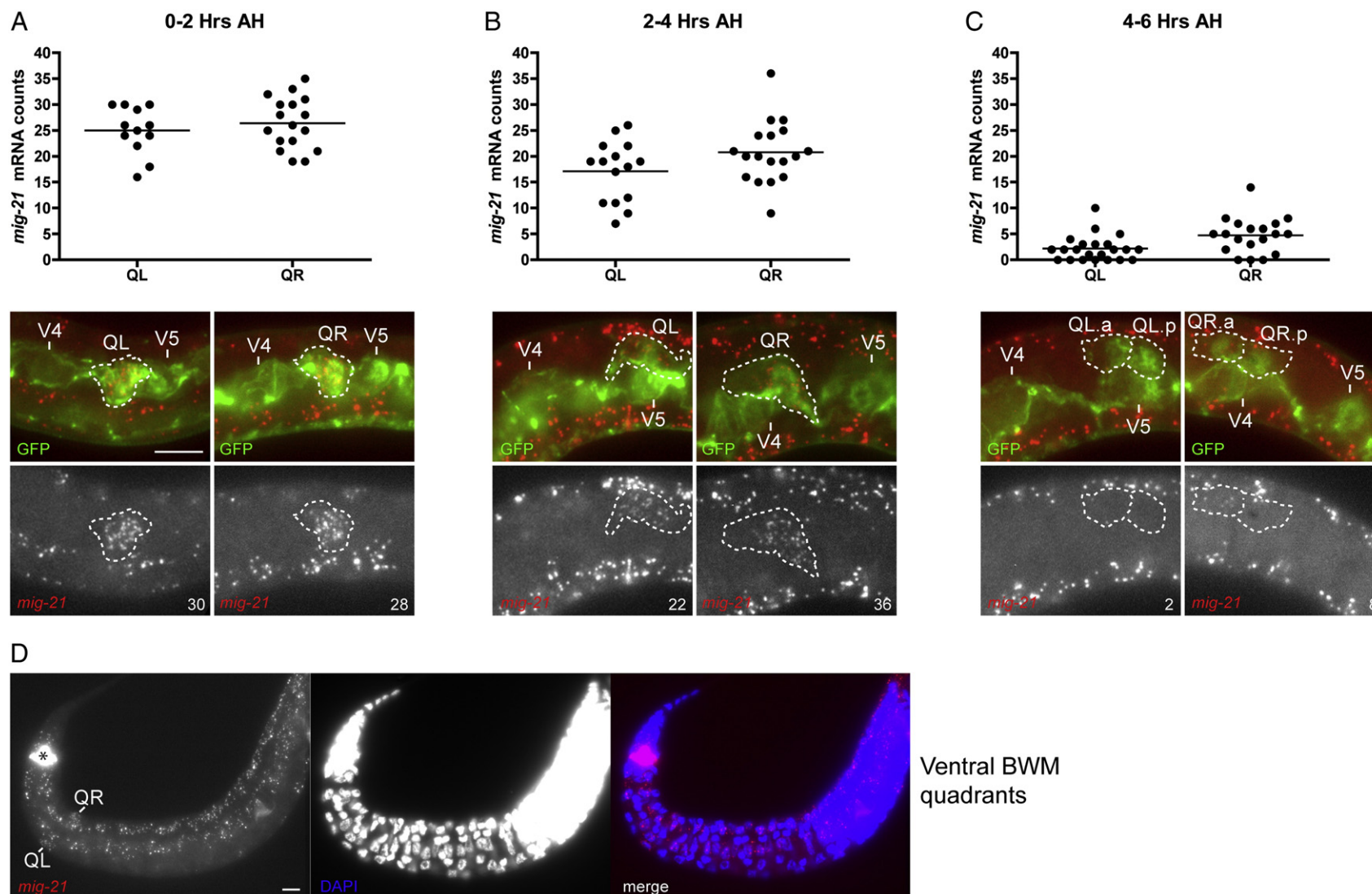


Fig. 4. Endogenous *mig-21* expression pattern. (A–C) Endogenous *mig-21* expression pattern during initial Q neuroblast migration analyzed by smFISH. Q cell specific expression was quantified in *helis63* animals synchronized 0–2 h (A), 2–4 h (B) or 4–6 h (C) after hatching. Quantifications were performed on z-stacks with a 0.5 μ m step size. Since spot intensities vary, only fluorescent spots that were visible in at least two adjacent z-slices were counted as single mRNA molecules. Micrographs show single z-slices. Numbers indicate the number of *mig-21* smFISH spots counted in the Q neuroblasts shown (using the entire z-stack). Lower panels: *mig-21* smFISH signal (red), upper panels: merged images with the GFP signal (green). Dashed line indicates the Q neuroblast outline, as identified by the GFP-PH marker. (D) Ventral view of *helis63* animals stained for *mig-21* mRNA using smFISH. DAPI counterstaining (blue) and a merged image are shown in the middle and right panel. *mig-21* expression is observed in body wall muscle quadrants along the anteroposterior axis. The position of QR and QL is indicated. The asterisk indicates the *Plin-48::Tomato* transgenic marker present in *helis63*. Scale bars represent 5 μ m for all micrographs. Anterior is left, dorsal is up.

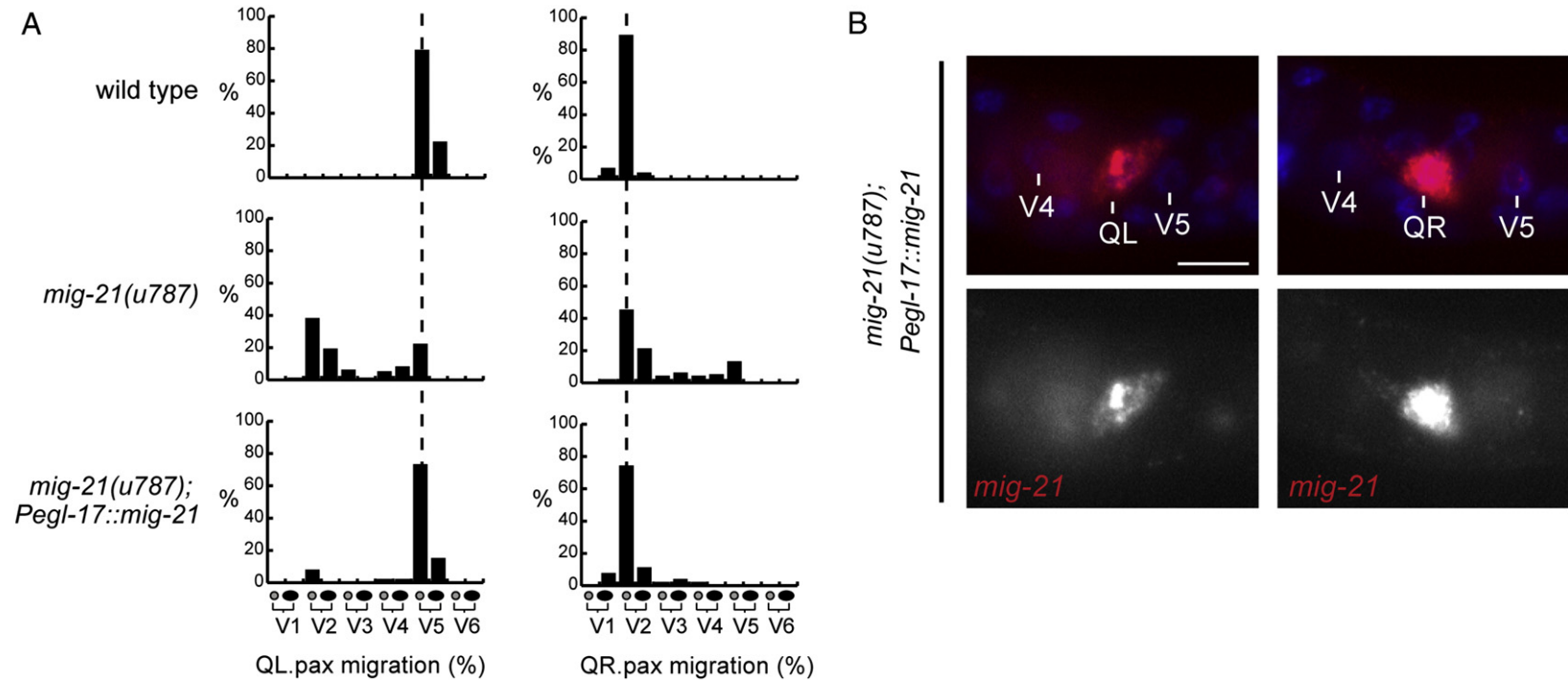


Fig. 5. *mig-21* acts cell autonomously in Q neuroblasts. (A) Quantification of the final positions of the Q.pax cells with respect to the stationary seam cells in wild type, *mig-21* and *mig-21; Pegl-17::mig-21* ($n > 80$ for wild type and *mig-21*, $n > 50$ for *mig-21; Pegl-17::mig-21*). (B) *mig-21* mRNA expression in QL and QR in animals carrying *Pegl-17::mig-21*. Lower panels show the *mig-21* smFISH signal (red) and the upper panels show merged images with DAPI nuclear counterstaining (blue). Q and seam cells were identified using nuclear counterstaining. Note that single *mig-21* transcripts cannot be distinguished due to overexpression of the *Pegl-17::mig-21* transgene. Scale bar represents 5 μm . Anterior is left, dorsal is up.

migration of the QL descendants toward the posterior (Harris et al., 1996; Salser and Kenyon, 1992). QR does not activate canonical Wnt/ β -catenin signaling and *mab-5* expression and as a consequence, the QR.d migrate in the default anterior direction. In *mig-21* mutants, a fraction of both the QL and QR descendants localize in the posterior (Fig. 1C). To investigate whether this posterior localization depends on EGL-20, we compared *egl-20* single and *mig-21*; *egl-20* double mutants. In *egl-20* mutants, canonical Wnt/ β -catenin signaling and *mab-*

5 expression is not activated in QL and the QL.d migrate toward the anterior. Also in *mig-21*; *egl-20* double mutants, all Q.d cells localized in the anterior, indicating that the posterior localization of the Q descendants in *mig-21* depends on EGL-20 signaling (Fig. 6A).

It has previously been shown that the left–right asymmetry in the response of QL and QR to EGL-20 is mediated through a difference in activation threshold for canonical Wnt/ β -catenin signaling and *mab-5* expression (Whangbo and Kenyon, 1999). As the QL and QR

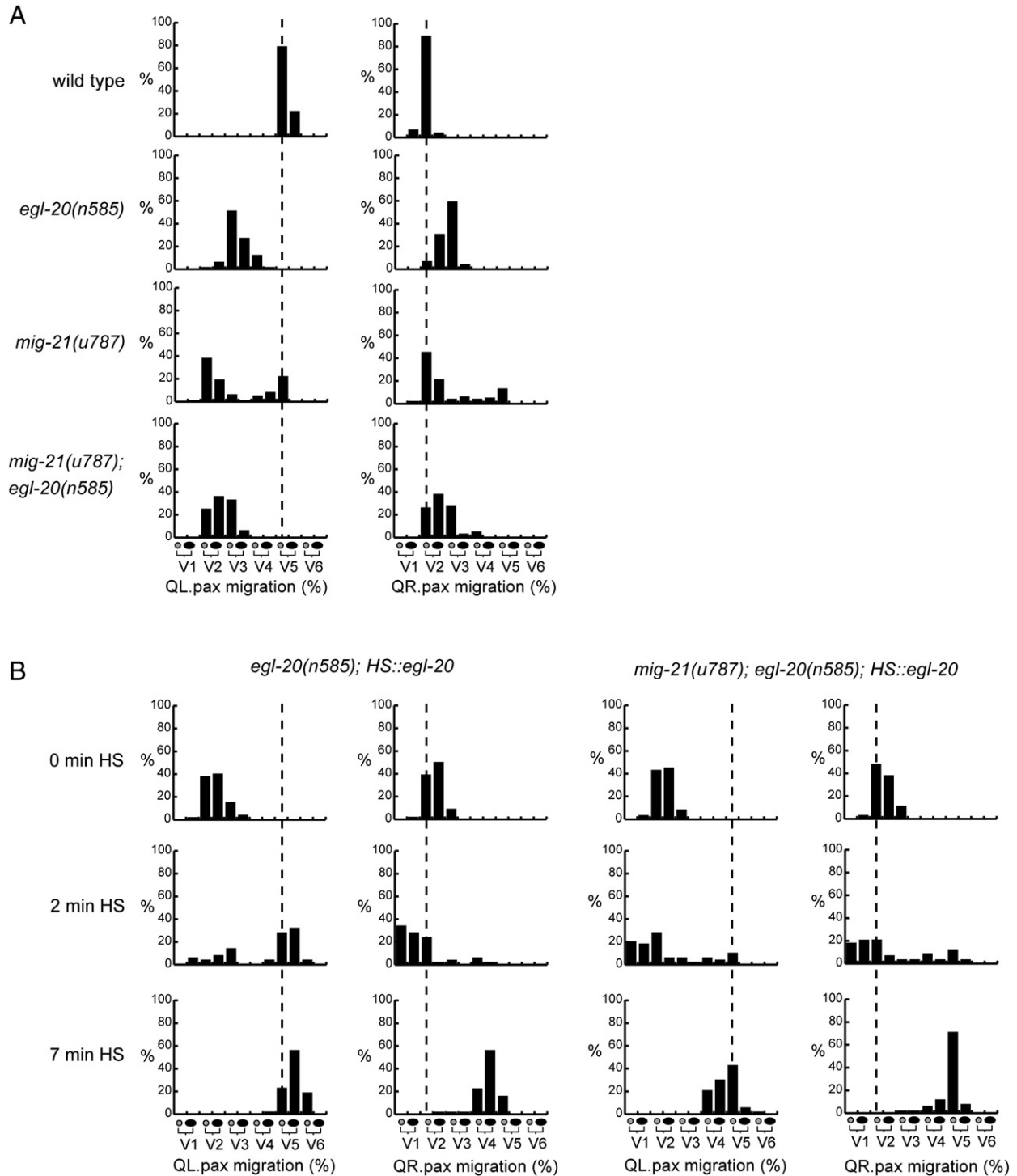


Fig. 6. *mig-21* is required for the left–right asymmetry in the response of the Q neuroblasts to the Wnt EGL-20. (A) Quantification of the final positions of the Q-pax cells with respect to the stationary seam cells in wild type, *mig-21*, *egl-20* and *mig-21*; *egl-20* mutants ($n > 80$ for wild type, *mig-21* and *mig-21*; *egl-20*, $n > 60$ for *egl-20*). (B) Quantification of the final positions of Q-pax cells with respect to the stationary seam cells in *egl-20*; *Phs::egl-20* (left diagrams) and *mig-21*; *egl-20*; *Phs::egl-20* (right diagrams) animals after 0, 2 and 7 minute heat shock pulses ($n \geq 50$ for all conditions).

neuroblasts appear to randomly activate canonical Wnt/ β -catenin signaling in *mig-21* mutants, we investigated whether the left–right asymmetry in EGL-20 response threshold is lost in *mig-21* mutants. To assay canonical Wnt/ β -catenin pathway activation by EGL-20, we expressed EGL-20 at different levels using a heat-inducible promoter in *egl-20* single mutants or *mig-21*; *egl-20* double mutants and determined the final position of the QL.d and QR.d (Fig. 6B). Without heat-shock, all Q descendants localized in the anterior in both the *egl-20* single and a *mig-21*; *egl-20* double mutant background. After a 7 minute heat-shock, all Q descendants localized in the posterior, indicating that at these expression levels, EGL-20 activated canonical Wnt/ β -catenin signaling in both QL and QR. However, after 2 min of heat-shock, 68% of the QL.d and 8% of the QR.d localized in the posterior in the *egl-20* control animals, consistent with the lower activation threshold of QL for canonical Wnt/ β -catenin signaling. In contrast, this left–right asymmetry in response to EGL-20 was lost in the *mig-21*; *egl-20* double mutants, with animals showing a similar distribution of the QL.d and QR.d along the anteroposterior axis (Fig. 6B). These results demonstrate that *mig-21* is required for the left–right asymmetry in the response to EGL-20 signaling.

Posterior polarization and migration of the Q neuroblasts is required for *mab-5* expression

Previous studies have suggested that the initial posterior migration of the Q neuroblasts correlates with the subsequent posterior migration of the Q descendants (Du and Chalfie, 2001; Honigberg and Kenyon, 2000). To address whether the initial posterior migration correlates with canonical Wnt/ β -catenin pathway activation, we examined expression of the Wnt target gene *mab-5* in Q neuroblasts after initial migration but before Q.d cell migration. Expression of *mab-5* was quantified using smFISH in Q neuroblasts and was plotted against the position of the Q neuroblasts on the anteroposterior axis. In wild type animals, *mab-5* was expressed at an average of 30 ± 7.1 (mean \pm SD,

$n = 32$) transcripts per cell in QL, and 3 ± 2.9 transcripts per cell in QR ($n = 28$) (Fig. 7A). Consistent with the finding that the left–right asymmetry in Wnt signaling response is lost in *mig-21* mutants, we found that the average *mab-5* expression level was similar in QL and QR ($p > 0.1$, t -test). Importantly, we observed that *mab-5* expression correlated with the position of the Q neuroblasts on the anteroposterior axis after initial migration (Spearman's rank correlation coefficient: QL, $r = 0.6709$, $n = 34$, $p < 10^{-4}$; QR, $r = 0.7529$, $n = 29$, $p < 10^{-5}$) (Fig. 7B). Thus, *mab-5* transcript counts were significantly higher in posteriorly positioned Q neuroblasts than in Q neuroblasts that had migrated toward the anterior. These results indicate that posterior localization of the Q neuroblasts is necessary for the EGL-20 dependent activation of *mab-5* expression. To further investigate this possibility, we measured *mab-5* transcript levels in the *unc-40*; *mig-21* double mutants discussed above, in which the Q neuroblasts fail to polarize and migrate posteriorly. We found that *mab-5* expression was not upregulated in *unc-40*; *mig-21* double mutants. Indeed, with transcript counts of 3 ± 2.0 for QL ($n = 13$) and 4 ± 3.4 for QR ($n = 19$), *mab-5* expression levels were similar as in wild type QR neuroblasts (Fig. 7C). As expected, this resulted in a complete loss of posterior Q.d migration (Fig. 2B).

Taken together, our results are consistent with a model in which the initial left–right asymmetric polarization and migration of the Q neuroblasts determines the difference in response to EGL-20. Posterior polarization and migration lowers the threshold for canonical Wnt/ β -catenin signaling, leading to specific expression of *mab-5* in the left Q cell lineage, while anterior polarization and migration ensures that *mab-5* remains off in the QR lineage. By controlling the initial polarization and migration of the Q neuroblasts, MIG-21 plays a central role in determining this left–right asymmetry in Wnt signaling response.

Discussion

During the development of complex multi-cellular organisms, cells need to communicate with each other to coordinate the

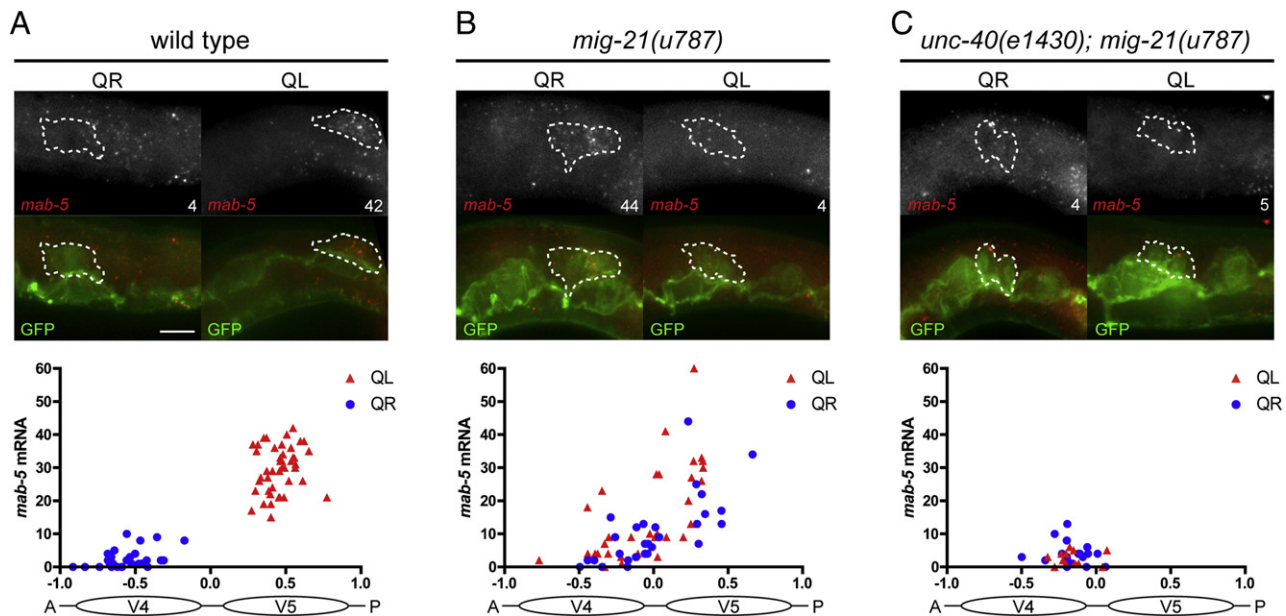


Fig. 7. Q neuroblast position and *mab-5* expression levels. Quantification of *mab-5* expression by smFISH in Q neuroblasts after initial migration in wild type (A), *mig-21* (B) and *unc-40*; *mig-21* (C) mutants carrying *hels63*. *mab-5* mRNA counts were plotted against the position of Q neuroblasts with respect to the seam cells V4 and V5. On the x-axis “-0.5” and “0.5” correspond to the position of the V4 and V5 nuclei, respectively. For quantification, z-stacks were used with a step size of 0.5 μ m. Since spot intensities vary, only fluorescent spots that were visible in at least two adjacent z-slices were counted as single mRNA molecules. Micrographs show single z-slices. Numbers indicate the number of *mab-5* smFISH spots in the Q neuroblasts shown (using the entire z-stack). The *mab-5* smFISH signal (red) is shown in top panels. Bottom panels show merged images with the GFP channel (GFP-PH and H2B-GFP, green). Dashed lines mark Q neuroblasts. Scale bars represent 5 μ m. Anterior is left, dorsal is up. To assess the correlation between *mab-5* transcript level and Q neuroblast position in *mig-21* mutants, we calculated the Spearman's rank correlation coefficients and found significant correlation between the two in both QL and QR (see main text for exact values). Furthermore, we performed robust linear regression to test whether a simple linear model could explain such correlation and found that this is indeed the case (QL: $y = 26.5x + 2.3$, $R^2 = 0.44$, $F = 18.39$, $p < 0.001$; QR: $y = 20.7x - 1.2$, $R^2 = 0.70$, $F = 25.26$, $p < 0.0001$).

formation of tissues and organs. A family of signaling molecules that plays a central role in development are the Wnt proteins, which control processes as diverse as cell fate specification and cell migration by triggering different intracellular signaling cascades. How target cells are specified to select such different signaling responses is however still largely unknown. Here, we have studied the left–right asymmetric response of the *C. elegans* Q neuroblasts to the Wnt protein EGL-20. We show that a left–right asymmetric polarization of the Q neuroblasts is required for a difference in response threshold of the two Q neuroblasts, ensuring that canonical Wnt/ β -catenin signaling is only activated in the left Q neuroblast. We found that this polarization is controlled by the TSP-I repeat containing protein MIG-21, which functions together with UNC-40/DCC to restrict posterior polarization to one side and anterior polarization to the other side.

mig-21 controls the initial polarization and migration of the Q neuroblasts

We found that *mig-21* is required for the initial polarization and migration of the Q neuroblasts. In *mig-21* mutants, the Q neuroblasts still detach from the row of seam cells and form protrusions, but these protrusions are not persistently polarized toward the anterior or posterior, with repeated changes in direction during the initial polarization process. This ultimately results in a mispositioning of the Q neuroblasts, with cells localizing at random positions between the wild type anterior and posterior positions. We found that *mig-21* functions cell autonomously in the Q neuroblasts and smFISH expression analysis showed that *mig-21* is transiently expressed in the Q neuroblasts during the initial polarization and migration stage, consistent with the requirement of *mig-21* during this stage in the Q migration process. *mig-21* is expressed at similar levels in the left and right Q neuroblasts, indicating that its role in specifying the left–right asymmetry in Q neuroblast polarization is indirect, for example by functioning as a receptor for a left–right asymmetric cue.

mig-21 encodes a single-pass transmembrane protein with two extracellular TSP-I repeats, a motif that is also present in guidance receptors such as UNC-5 and Semaphorin (Adams and Tucker, 2000). UNC-5 functions as a co-receptor of UNC-40/DCC in dorsoventral axons guidance (Wadsworth, 2002). As MIG-21 shares the presence of TSP-I motifs with UNC-5, we hypothesized that MIG-21 may have a similar co-receptor function in Q neuroblast polarization. Our genetic results showing a strong synergistic effect of *unc-40* and *mig-21* indicate that the functional relationship between MIG-21 and UNC-40 is more complex. It should be noted, however, that also *unc-5* can function partially redundantly with *unc-40*, as UNC-5 and UNC-40 can partially substitute for each other in the guidance of the distal tip cells (Merz et al., 2001). Future studies will determine the functional relationship between MIG-21 and UNC-40. The guidance cues that control the left–right asymmetric polarization of the Q neuroblasts remain elusive. So far, no secreted molecules have been identified that affect the initial polarization and migration of the Q neuroblasts. Guidance may however also be mediated through direct cell–cell contact, for example with the V4 and V5 seam cells along which the Q neuroblasts polarize and migrate or with commissural axons that are located in close proximity to the migrating Q cells.

We found that *unc-40* is particularly important for the posterior polarization of the Q neuroblasts. Thus, in *unc-40* single mutants, there is an anterior shift in the localization of the QL neuroblasts, whereas the extent of the anterior migration of the QR neuroblasts is only slightly affected. This reduction in posterior localization is even more pronounced in *unc-40*; *mig-21* double mutants, with none of the Q neuroblasts extending to positions over seam cell V5. These results are consistent with a model in which *unc-40* is necessary for posterior polarization and migration of the Q neuroblasts. A similar function of *unc-40* has been shown in axon guidance, where overexpression of *unc-40* was sufficient to reorient pioneering axons toward the posterior (Levy-Strumpf and Culotti, 2007). The posterior polarization and migration of the Q neuroblasts is also strongly reduced in double mutants between *unc-40* and *dpy-19*,

indicating that *mig-21* and *dpy-19* may act in the same pathway (Honigberg and Kenyon, 2000). In support of this notion is our observation that the Q,d migration phenotype of *mig-21 dpy-19* double mutants is similar to the phenotype of the single mutants (Fig. S3). *dpy-19* encodes a novel but evolutionarily conserved transmembrane protein. Interestingly, studies on the mammalian ortholog have shown that mDPY-19 is expressed in neuronal progenitor cells in the brain (Kurokawa et al., 2005), indicating that the function of DPY-19 in neuroblast polarization may be a conserved feature of nervous system development.

Polarization direction determines the threshold for EGL-20 dependent canonical Wnt/ β -catenin signaling

It has previously been shown that a difference in response threshold to EGL-20 determines that canonical Wnt/ β -catenin signaling is only activated in QL (Whangbo and Kenyon, 1999). This ensures that expression of the EGL-20 target gene *mab-5* is restricted to QL and leads to the opposite migration of the QL and QR descendants. We found that the difference in response threshold to EGL-20 is lost in *mig-21* mutants, indicating that the initial left–right asymmetric polarization and migration of the Q neuroblasts is linked to the subsequent difference in EGL-20 signaling.

Using smFISH analysis, we show that there is a clear correlation between the final position of the Q neuroblasts and EGL-20 signaling activity, as measured by the expression level of *mab-5*. Thus, in wild type animals, only the posteriorly localized QL neuroblasts express *mab-5*. In *mig-21* mutants, in which the positioning of the QL and QR neuroblasts is random, there is also a clear correlation with posterior localization and *mab-5* expression, with the most posteriorly localized QL and QR cells showing the highest *mab-5* transcript count. Importantly, we found that posterior localization is essential for *mab-5* expression, as *mab-5* fails to be upregulated in *unc-40*; *mig-21* double mutants in which posterior migration of the Q neuroblasts is absent. Taken together, these results are consistent with a model in which posterior localization of the Q neuroblasts lowers the threshold for the EGL-20 dependent expression of *mab-5*.

How would the initial posterior polarization and migration sensitize QL for canonical EGL-20 signaling? As EGL-20 is expressed in the tail and forms a posterior to anterior concentration gradient (Coudreuse et al., 2006; Whangbo and Kenyon, 1999), posterior polarization and migration may simply expose QL to a higher level of EGL-20. This higher level of EGL-20 will then specifically trigger canonical Wnt/ β -catenin signaling and *mab-5* expression in QL. An argument against such a model is that the difference in response threshold to EGL-20 can also be observed when EGL-20 is expressed ubiquitously using a heat-shock promoter. Furthermore, when the EGL-20 concentration gradient is reversed, the left–right asymmetry in Q descendant migration is still partially maintained (Whangbo and Kenyon, 1999). An alternative possibility is that posterior migration exposes QL to a localized cue that modulates the responsiveness to EGL-20, for example by influencing the expression of Wnt receptors or intracellular signaling components such as the rate limiting negative regulator Axin (Lee et al., 2003).

Taken together, our results show that the Q neuroblasts are specified to respond differently to Wnt through a process that involves a left–right asymmetric polarization and short range migration. Future studies will address how this asymmetry defines the threshold for canonical Wnt/ β -catenin signaling.

Supplementary materials related to this article can be found online at doi:10.1016/j.ydbio.2011.10.029.

Acknowledgments

We thank Dr. M. Wildwater and Dr. S. van den Heuvel for *hels63*, Dr. Guanshuo Ou for advise on live imaging, Dr. Andrew Fire for expression vectors, the *Caenorhabditis* Genetic Center (University of

Minnesota, Minneapolis) for strains and the Hubrecht Imaging Center (HIC) for assistance with imaging. This work was funded by a grant from the Dutch Cancer Society (HUBR 2008-4114) to H.C.K.

References

- Adams, J.C., Tucker, R.P., 2000. The thrombospondin type 1 repeat (TSR) superfamily: diverse proteins with related roles in neuronal development. *Dev. Dyn.* 218, 280–299.
- Branda, C.S., Stern, M.J., 2000. Mechanisms controlling sex myoblast migration in *Caenorhabditis elegans* hermaphrodites. *Dev. Biol.* 226, 137–151.
- Brenner, S., 1974. The genetics of *Caenorhabditis elegans*. *Genetics* 77, 71–94.
- Cadigan, K.M., Nusse, R., 1997. Wnt signaling: a common theme in animal development. *Genes Dev.* 11, 3286–3305.
- Chapman, J.O., Li, H., Lundquist, E.A., 2008. The MIG-15 NIK kinase acts cell-autonomously in neuroblast polarization and migration in *C. elegans*. *Dev. Biol.* 324, 245–257.
- Ch'ng, Q., Williams, L., Lie, Y.S., Sym, M., Whangbo, J., Kenyon, C., 2003. Identification of genes that regulate a left–right asymmetric neuronal migration in *Caenorhabditis elegans*. *Genetics* 164, 1355–1367.
- Clevers, H., 2006. Wnt/ β -catenin signaling in development and disease. *Cell* 127, 469–480.
- Cordes, S., Frank, C.A., Garriga, G., 2006. The *C. elegans* MELK ortholog PIG-1 regulates cell size asymmetry and daughter cell fate in asymmetric neuroblast divisions. *Development* 133, 2747–2756.
- Coudreuse, D.Y., Roel, G., Betist, M.C., Destree, O., Korswagen, H.C., 2006. Wnt gradient formation requires retromer function in Wnt-producing cells. *Science* 312, 921–924.
- Du, H., Chalfie, M., 2001. Genes regulating touch cell development in *Caenorhabditis elegans*. *Genetics* 158, 197–207.
- Gu, T., Orita, S., Han, M., 1998. *Caenorhabditis elegans* SUR-5, a novel but conserved protein, negatively regulates LET-60 Ras activity during vulval induction. *Mol. Cell Biol.* 18, 4556–4564.
- Harris, J., Honigberg, L., Robinson, N., Kenyon, C., 1996. Neuronal cell migration in *C. elegans*: regulation of Hox gene expression and cell position. *Development* 122, 3117–3131.
- Honigberg, L., Kenyon, C., 2000. Establishment of left/right asymmetry in neuroblast migration by UNC-40/DCC, UNC-73/Trio and DPY-19 proteins in *C. elegans*. *Development* 127, 4655–4668.
- Kamath, R.S., Ahringer, J., 2003. Genome-wide RNAi screening in *Caenorhabditis elegans*. *Methods* 30, 313–321.
- Kamath, R.S., Fraser, A.G., Dong, Y., Poulin, G., Durbin, R., Gotta, M., Kanapin, A., Le Bot, N., Moreno, S., Sohrmann, M., Welchman, D.P., Zipperlen, P., Ahringer, J., 2003. Systematic functional analysis of the *Caenorhabditis elegans* genome using RNAi. *Nature* 421, 231–237.
- Korswagen, H.C., Herman, M.A., Clevers, H.C., 2000. Distinct β -catenins mediate adhesion and signalling functions in *C. elegans*. *Nature* 406, 527–532.
- Kurokawa, K., Tamura, Y., Kataoka, Y., Yamada, H., Nakamura, T., Taki, K., Kudo, M., 2005. A mammalian *dpy-19* homologue is expressed in GABAergic neurons. *Med. Mol. Morphol.* 38, 79–83.
- Lee, E., Salic, A., Kruger, R., Heinrich, R., Kirschner, M.W., 2003. The roles of APC and Axin derived from experimental and theoretical analysis of the Wnt pathway. *PLoS Biol.* 1, E10.
- Levy-Strumpf, N., Culotti, J.G., 2007. VAB-8, UNC-73 and MIG-2 regulate axon polarity and cell migration functions of UNC-40 in *C. elegans*. *Nat. Neurosci.* 10, 161–168.
- Malooof, J.N., Whangbo, J., Harris, J.M., Jongeward, G.D., Kenyon, C., 1999. A Wnt signaling pathway controls Hox gene expression and neuroblast migration in *C. elegans*. *Development* 126, 37–49.
- Merz, D.C., Zheng, H., Killeen, M.T., Krizus, A., Culotti, J.G., 2001. Multiple signaling mechanisms of the UNC-6/netrin receptors UNC-5 and UNC-40/DCC in vivo. *Genetics* 158, 1071–1080.
- Raj, A., van den Bogaard, P., Rifkin, S.A., van Oudenaarden, A., Tyagi, S., 2008. Imaging individual mRNA molecules using multiple singly labeled probes. *Nat. Methods* 5, 877–879.
- Salsler, S.J., Kenyon, C., 1992. Activation of a *C. elegans* Antennapedia homologue in migrating cells controls their direction of migration. *Nature* 355, 255–258.
- Schlessinger, K., Hall, A., Tolwinski, N., 2009. Wnt signaling pathways meet Rho GTPases. *Genes Dev.* 23, 265–277.
- Sulston, J.E., Horvitz, H.R., 1977. Post-embryonic cell lineages of the nematode, *Caenorhabditis elegans*. *Dev. Biol.* 56, 110–156.
- Wadsworth, W.G., 2002. Moving around in a worm: netrin UNC-6 and circumferential axon guidance in *C. elegans*. *Trends Neurosci.* 25, 423–429.
- Whangbo, J., Kenyon, C., 1999. A Wnt signaling system that specifies two patterns of cell migration in *C. elegans*. *Mol. Cell* 4, 851–858.
- Williams, B.D., Schrank, B., Huynh, C., Shownkeen, R., Waterston, R.H., 1992. A genetic mapping system in *Caenorhabditis elegans* based on polymorphic sequence-tagged sites. *Genetics* 131, 609–624.
- Zinovyeva, A.Y., Yamamoto, Y., Sawa, H., Forrester, W.C., 2008. Complex network of Wnt signaling regulates neuronal migrations during *Caenorhabditis elegans* development. *Genetics* 179, 1357–1371.